AIAA JOURNAL
Vol. 37, No. 5, May 1999

Element Stress Recovery Technique with Equilibrium Constraints for Superconvergent Boundary Stress Extraction

Hoon Cheol Park* and Sahng-Hoon Shin†
Konkuk University, Seoul 143-701, Republic of Korea

An element stress recovery technique is proposed for accurate boundary stress extraction. The equilibrium constraint is imposed using two residuals of the equilibrium in variational forms. For the recovery stress fields, only a dominant stress component is assumed as higher order, and all other components are assumed as high as the order of the assumed displacement in the finite element used for the stress analysis. The recovery stress fields are postulated within an element, whereas they are assumed over an element patch in the patch stress recovery technique. By employing these features, the final matrix to be inverted becomes well conditioned. Numerical examples have demonstrated that quite accurate boundary stresses can be recovered even for coarse meshes using the proposed method. It is also shown that the method can accurately extract boundary stresses without implementing the superconvergent stresses. The method should be very effective for localized boundary stress extraction.

Introduction

In the development of a finite element program for stress analysis, a routine for the stress calculation should be included as the final stage of the program. However, it is not easy to develop a satisfactory stress recovery routine because the stresses calculated in the finite element method are not continuous across elements. Moreover, the calculated stresses are accurate only at some special sampling points, such as the Gauss integration points and the so-called superconvergent points. At these points, the stresses have higher accuracy than at any other points within an element. Balow[1] showed the existence of such optimal points inside of various types of elements.

Since the 1970s many researchers[2–5] have attempted to develop better stress recovery techniques. Recently, the so-called patch recovery technique or the Zienkiewicz–Zhu (ZZ) method[6,7] has become an influence on a new trend in the development of the stress recovery scheme due to its implementation simplicity. In this method, the stresses calculated at the optimal points or the superconvergent points in an element patch are used to obtain a continuous stress field over the patch. Because the order of the assumed stress field of the patch is strictly dependent on the number of the superconvergent points within the patch, only a low-order stress field can be assumed for the recovery stress. As a result, the recovered stresses at the grid points that are included in only one patch have poor accuracy. Because these grid points are usually located at the boundaries of a finite element model, the inaccurately recovered stresses may cause dangerous results when the stresses are used for design optimization.

New ideas have been introduced[8–11] to resolve this problem. The common idea of these approaches is to improve the accuracy of the recovery stress within a patch by increasing the order of the assumed stress field. However, this may cause an ill-conditioned matrix in the final stage of the patch stress recovery routine inasmuch as the order of the assumed stress field is limited by the number of the superconvergent stresses within the patch. To overcome this drawback, the equilibrium constraint has been introduced into the ZZ method in various ways, and the order of the assumed stress polynomial has been increased.

Wiberg and Abdulwahab[8] and Wiberg et al.[9] proposed a patch stress recovery technique that can increase the order of the assumed stress field by imposing an equilibrium constraint. In their work, the equilibrium constraint was applied such that the assumed stress can minimize the squares of residuals of the equilibrium equation.[8,9] Some improvement in the accuracy of the recovery stress was achieved by this method. Blacker and Belytschko[10] implemented squares of the equilibrium residuals and included the norm of the traction boundary residual in the error functional to be minimized. They[10] also introduced the conjoint polynomial to enhance the accuracy of the recovery stresses in overlapping patches, and slight improvement in the rate of convergence was achieved. As another way to implement an equilibrium constraint in the patch recovery technique, Lee et al.[11] used a virtual work form of the equilibrium residual, called the Lee–Park (LP) method. In the LP method, the patch residual of the equilibrium was formulated based on the principle of virtual work and included in the error functional for minimization. In the formulation, the traction was calculated in terms of the patch stiffness, and the displacement was obtained from the finite element analysis. Boroomand and Zienkiewics[12] demonstrated that an accurate stress recovery is possible even without implementing the superconvergent stresses for some particular examples. In spite of this intensive research, significant accuracy improvement in the recovered boundary stresses has not been reported.

A method of element stress recovery is proposed to improve the accuracy of the boundary stresses called the Shin–Park (SP) method. This method employs the basic concepts from the previous LP method,[11] but the stress is recovered by each element. In addition to the equilibrium residual formulated in the LP method, an additional residual is derived from the principle of virtual work by representing traction forces in terms of the assumed stress field within each element. The order of the assumed stress component is selectively chosen to be equal to or higher than that of the displacement field assumed in the finite element used for the stress analysis. Because at least one of the stress components is assumed as higher than that of the assumed displacement, higher-order elements are used for the construction of matrices in the present technique. These new features have resulted in a well-conditioned final matrix to be inverted.

Test examples, including a three-dimensional problem, have demonstrated satisfactory enhancement in the accuracy of the recovered boundary stress in comparison with results from the ZZ method, the modified LP method, and the element-by-element extrapolation denoted as average (AVG) in this paper.

Formulation

In the present technique, contrary to previous patch recoveries,[6–11] the stress field is assumed at each element and is expressed as

$$\boldsymbol{\sigma}_e = \boldsymbol{P}\boldsymbol{a} \tag{1}$$

where $\boldsymbol{\sigma}_e$ is the assumed stress vector in an element, $\boldsymbol{P}$ is the polynomial matrix, and $\boldsymbol{a}$ is the coefficient vector to be determined. For

Received Jan. 6, 1998; presented as Paper 98-1712 at the AIAA/ASME/ASCE/AHS/ASC 39th Structures, Structural Dynamics, and Materials Conference, Long Beach, CA, April 20–23, 1998; revision received Jan. 5, 1999; accepted for publication Jan. 9, 1999.

*Assistant Professor, Department of Aerospace Engineering. Member AIAA.

†Graduate Student, Department of Aerospace Engineering; currently Engineer, Technical Center, Koryo, Ltd., 493 Kajwa-dong, Seo-ku, Incheon 404-254, Republic of Korea.

one-dimensional problems, in which case the stress field has only one component, the $\boldsymbol{P}$ matrix can be expressed as

$$\boldsymbol{P} = [1 \quad \xi \quad \xi^2] \tag{2}$$

when the stress is assumed as a quadratic polynomial in terms of the parent coordinate ξ and the vector $\boldsymbol{a}$ has three undetermined coefficients. When linear elements are used for the one-dimensional problem, the order of this assumed stress becomes higher than that of the assumed displacement for the linear element.

For two-dimensional problems, the $\boldsymbol{P}$ matrix should be written as

$$\boldsymbol{P} = \begin{bmatrix} \bar{\boldsymbol{P}}_1 & \boldsymbol{0} & \boldsymbol{0} \\ \boldsymbol{0} & \bar{\boldsymbol{P}}_2 & \boldsymbol{0} \\ \boldsymbol{0} & \boldsymbol{0} & \bar{\boldsymbol{P}}_3 \end{bmatrix} \tag{3}$$

because the stress field has three components. Here $\bar{\boldsymbol{P}}_1, \bar{\boldsymbol{P}}_2, \bar{\boldsymbol{P}}_3$ can be assumed as either

$$\bar{\boldsymbol{P}}_i = [1 \quad \xi \quad \eta \quad \xi\eta], \qquad i = 1, 2, 3 \tag{4}$$

or

$$\bar{\boldsymbol{P}}_i = [1 \quad \xi \quad \eta \quad \xi^2 \quad \xi\eta \quad \eta^2], \qquad i = 1, 2, 3 \tag{5}$$

depending on which component is dominant. When elements with the bilinear displacement field are used for the finite element analysis, the assumed stress in Eq. (4) has the same order of that of the assumed displacement. If the assumed stress in Eq. (5) is used, the order of the assumed stress becomes higher than that of the assumed displacement in the bilinear element.

In other words, the order of each assumed stress component can be equal to or higher than that of the displacement field assumed in the finite element used for analysis. This is one of the important considerations to produce a well-conditioned final matrix, especially for the three-dimensional stress recovery problem in which six stress components must be assumed at a time. This selective higher-order stress assumption will be demonstrated in the following section.

The general expression for the difference between the stress calculated from the assumed recovery stress field $\boldsymbol{\sigma}_e$ and the stress obtained by the finite element analysis $\boldsymbol{\sigma}_h$ at the ith superconvergent point inside of an element can be expressed as

$$\begin{aligned} \boldsymbol{e}_i &= \boldsymbol{\sigma}_e(\xi_i, \eta_i, \zeta_i) - \boldsymbol{\sigma}_h(\xi_i, \eta_i, \zeta_i) \\ &= \boldsymbol{P}(\xi_i, \eta_i, \zeta_i)\boldsymbol{a} - \boldsymbol{\sigma}_h(\xi_i, \eta_i, \zeta_i) \end{aligned} \tag{6}$$

where (ξ_i, η_i, ζ_i) represents the parent coordinates of the ith superconvergent point.

A solid in an equilibrium state satisfies the following equation, which stands for the well-known principle of virtual work:

$$\delta\pi = \int_V \delta\boldsymbol{\varepsilon}^T \boldsymbol{\sigma}\, \mathrm{d}V - \int_S \delta\boldsymbol{u}^T \bar{\boldsymbol{T}}\, \mathrm{d}S - \int_V \delta\boldsymbol{u}^T \boldsymbol{f}\, \mathrm{d}V = 0 \tag{7}$$

where $\delta\boldsymbol{\varepsilon}$ is the virtual strain vector, $\boldsymbol{\sigma}$ is the stress vector, $\delta\boldsymbol{u}$ is the virtual displacement vector, $\bar{\boldsymbol{T}}$ is the traction force vector, $\boldsymbol{f}$ is the body force vector, V is the volume of interest, and S is the surface under the traction force.

Because the actual stress is unknown, the actual stress $\boldsymbol{\sigma}$ is replaced by the assumed stress field $\boldsymbol{\sigma}_e$ at each element, and the traction term $\bar{T}$ is expressed in terms of the assumed stress $\boldsymbol{\sigma}_e$ as follows:

$$(\delta\pi_{\text{res}})_1 = \int_{V_e} \delta\boldsymbol{\varepsilon}^T \boldsymbol{\sigma}_e\, \mathrm{d}V - \int_{S_e} \delta\boldsymbol{u}^T \boldsymbol{L}\boldsymbol{\sigma}_e\, \mathrm{d}S - \int_{V_e} \delta\boldsymbol{u}^T \boldsymbol{f}\, \mathrm{d}V \tag{8}$$

where V_e is the volume of an element and $\boldsymbol{L}$ is the direction cosine matrix that represents normal directions of each element boundary surface S_e. The sum of each element residual of equilibrium $(\delta\pi_{\text{res}})_1$ does not approach zero until the assumed stress field is very close to the actual stress.

The virtual displacement vector $\delta\boldsymbol{u}$ can be interpolated using the virtual element nodal degree-of-freedom (DOF) vector $\delta\boldsymbol{q}_e$, and the virtual strain vector $\delta\boldsymbol{\varepsilon}$ can be obtained by differentiating the virtual element nodal DOF vector $\delta\boldsymbol{q}_e$ in the following way:

$$\delta\boldsymbol{u} = \boldsymbol{N}\delta\boldsymbol{q}_e, \qquad \delta\boldsymbol{\varepsilon} = \boldsymbol{B}\delta\boldsymbol{q}_e \tag{9}$$

where $\boldsymbol{N}$ is the shape function matrix and $\boldsymbol{B}$ is the operation matrix that relates the strain and displacement within an element. Introducing Eqs. (1) and (9) into the first term in the right-hand side of Eq. (8), the following expression is obtained:

$$\int_{V_e} \delta\boldsymbol{\varepsilon}^T \boldsymbol{\sigma}_e\, \mathrm{d}V = \delta\boldsymbol{q}_e^T \boldsymbol{C}_e \boldsymbol{a} \tag{10}$$

where

$$\boldsymbol{C}_e = \int_{V_e} \boldsymbol{B}^T \boldsymbol{P}\, \mathrm{d}V$$

The second and third term in the right-hand side of Eq. (8) can be written as

$$\int_{S_e} \delta\boldsymbol{u}^T \boldsymbol{L}\boldsymbol{\sigma}_e\, \mathrm{d}S + \int_{V_e} \delta\boldsymbol{u}^T \boldsymbol{f}\, \mathrm{d}V = \delta\boldsymbol{q}_e^T (\boldsymbol{D}_e\boldsymbol{a} + \boldsymbol{F}_b) \tag{11}$$

where

$$\boldsymbol{D}_e = \int_{S_e} \bar{\boldsymbol{N}}^T \boldsymbol{L}\boldsymbol{P}\, \mathrm{d}S, \qquad \boldsymbol{F}_b = \int_{V_e} \boldsymbol{N}^T \boldsymbol{f}\, \mathrm{d}V$$

and $\bar{\boldsymbol{N}}$ is the shape function matrix over the element boundary surface. Finally, using Eqs. (10) and (11), the residual of equilibrium $(\delta\pi_{\text{res}})_1$ in Eq. (8) can be rewritten as

$$(\delta\pi_{\text{res}})_1 = \delta\boldsymbol{q}_e^T [(\boldsymbol{C}_e - \boldsymbol{D}_e)\boldsymbol{a} - \boldsymbol{F}_b] = \delta\boldsymbol{q}_e^T (\boldsymbol{R}_{\text{eq}})_1 \tag{12}$$

where the first residual vector $(\boldsymbol{R}_{\text{eq}})_1$ is defined as $(\boldsymbol{R}_{\text{eq}})_1 = (\boldsymbol{C}_e - \boldsymbol{D}_e)\boldsymbol{a} - \boldsymbol{F}_b$.

The equilibrium residual of an element can be derived in a different way by representing the second and third terms in the right-hand side of Eq. (7) using the stiffness matrix of the element as follows:

$$\int_{S_e} \delta\boldsymbol{u}^T \bar{\boldsymbol{T}}\, \mathrm{d}S + \int_{V_e} \delta\boldsymbol{u}^T \boldsymbol{f}\, \mathrm{d}V = \delta\boldsymbol{q}_e^T \boldsymbol{F}_e = \delta\boldsymbol{q}_e^T \boldsymbol{K}_e \boldsymbol{q}_e \tag{13}$$

where $\boldsymbol{F}_e$ is the nodal load vector, $\boldsymbol{q}_e$ is the element nodal DOF vector obtained from the finite element analysis, and $\boldsymbol{K}_e$ is the element stiffness matrix formulated using the higher-order element. Therefore, another form of the residual of the equilibrium $(\delta\pi_{\text{res}})_2$ can be expressed as

$$(\delta\pi_{\text{res}})_2 = \int_{V_e} \delta\boldsymbol{\varepsilon}^T \sigma_e\, \mathrm{d}V - \delta\boldsymbol{q}_e^T \boldsymbol{K}_e \boldsymbol{q}_e = \delta\boldsymbol{q}_e^T (\boldsymbol{C}_e\boldsymbol{a} - \boldsymbol{F}_e) \tag{14}$$

where $\boldsymbol{C}_e$ is the same matrix obtained in Eq. (10). The $(\delta\pi_{\text{res}})_2$ in Eq. (14) can be simply written as the following equation:

$$(\delta\pi_{\text{res}})_2 = \delta\boldsymbol{q}_e^T (\boldsymbol{C}_e\boldsymbol{a} - \boldsymbol{F}_e) = \delta\boldsymbol{q}_e^T (\boldsymbol{R}_{\text{eq}})_2 \tag{15}$$

where the second residual vector $(\boldsymbol{R}_{\text{eq}})_2$ is defined as $(\boldsymbol{R}_{\text{eq}})_2 = \boldsymbol{C}_e\boldsymbol{a} - \boldsymbol{F}_e$.

The coefficient vector $\boldsymbol{a}$ is determined such that the stress error $\boldsymbol{e}_i$, the first residual vector $(\boldsymbol{R}_{\text{eq}})_1$, and the second residual vector $(\boldsymbol{R}_{\text{eq}})_2$ are minimized in the least-squares sense. Thus, the error functional $F(\boldsymbol{a})$ is constructed as

$$\begin{aligned} F(\boldsymbol{a}) &= \alpha \sum_{i=1}^{n} \boldsymbol{e}_i^T \boldsymbol{e}_i + \beta \left(\boldsymbol{R}_{\text{eq}}^T\right)_1 (\boldsymbol{R}_{\text{eq}})_1 + \gamma \left(\boldsymbol{R}_{\text{eq}}^T\right)_2 (\boldsymbol{R}_{\text{eq}})_2 \\ &= \alpha \sum_{i=1}^{n} (\boldsymbol{P}\boldsymbol{a} - \boldsymbol{\sigma}_h)^T (\boldsymbol{P}\boldsymbol{a} - \boldsymbol{\sigma}_h) + \beta [(\boldsymbol{C}_e - \boldsymbol{D}_e)\boldsymbol{a} - \boldsymbol{F}_b]^T \\ &\quad \times [(\boldsymbol{C}_e - \boldsymbol{D}_e)\boldsymbol{a} - \boldsymbol{F}_b] + \gamma [\boldsymbol{C}_e\boldsymbol{a} - \boldsymbol{F}_e]^T [\boldsymbol{C}_e\boldsymbol{a} - \boldsymbol{F}_e] \end{aligned} \tag{16}$$

where n is the total number of sampling points within an element and α, β, and γ are the penalty parameters. In Eq. (16), the first term of $F(\boldsymbol{a})$ corresponds to the least-squares functional used in the ZZ method.[6,7] The third term is in the same form as the residual

functional introduced in the LP method.[11] By employing the second term in addition to the third term, a higher-order stress field can be assumed within an element, and the accurate boundary stress is stably recovered, even for the three-dimensional problem.

The coefficient vector $\boldsymbol{a}$ in Eq. (1) is determined by minimizing the functional in Eq. (16) with respect to the coefficient vector. Thus, the coefficient vector $\boldsymbol{a}$ is obtained such that the following equation is satisfied:

$$\frac{\partial F(\boldsymbol{a})}{\partial \boldsymbol{a}} = 0 \tag{17}$$

After rearrangement this condition can be rewritten as follows:

$$\left[\alpha \sum_{i=1}^{n} \boldsymbol{P}^T \boldsymbol{P} + \beta(\boldsymbol{C}_e - \boldsymbol{D}_e)^T(\boldsymbol{C}_e - \boldsymbol{D}_e) + \gamma \boldsymbol{C}_e^T \boldsymbol{C}_e\right]\boldsymbol{a}$$

$$= \alpha \sum_{i=1}^{n} \boldsymbol{P}^T \boldsymbol{\sigma}_h + \beta(\boldsymbol{C}_e - \boldsymbol{D}_e)^T \boldsymbol{F}_b + \gamma \boldsymbol{C}_e^T \boldsymbol{F}_e \tag{18}$$

The final matrix in the bracket in front of the coefficient vector $\boldsymbol{a}$ becomes well conditioned even for zero α and for the three-dimensional stress recovery example in which all six stress components must be assumed at a time. Therefore, we can solve Eq. (18) by using a conventional Gaussian elimination solver for any problem.

When the original LP method was used to recover stresses for the in-plane bending problems (example 3 in the present paper), the final matrix became ill conditioned. As a result, a special solver based on singular value decompostion should be used to solve the final equation. Therefore, the LP method is modified such that the additional residual of the equilibrium [the term with γ in Eq. (18)] is implemented as in the SP method, and all of the stress components are assumed as higher order. This modified LP method is denoted as LP in the present paper.

Numerical examples will show that the recovered boundary stresses are relatively accurate compared with the boundary stresses obtained by the ZZ method, the modified LP method, and the conventional element stress extrapolation method. The abbreviation AVG stands for the bilinear element stress extrapolation in the two-dimensional problems and the trilinear element stress extrapolation in the three-dimensional problem.

Numerical Examples

Performance of the proposed method is demonstrated by the following four examples. In the one-dimensional example, two-node linear elements are used for the finite element analysis and three-node elements are adopted for the construction of the $\boldsymbol{B}$ matrix in Eq. (9) and $\boldsymbol{K}_e$ matrix in Eq. (13). Four-node plane stress elements with a bilinear displacement field are used for the two-dimensional stress analysis, and the eight-node plane stress element is used to build the $\boldsymbol{B}$ and $\boldsymbol{K}_e$ matrices. Similarly, the eight-node solid element is selected for the three-dimensional stress analysis and the 20-node element is used to construct the $\boldsymbol{B}$ and $\boldsymbol{K}_e$ matrices. Figure 1 summarizes this choice of element types for each example. The result from the present method is denoted as SP in all examples.

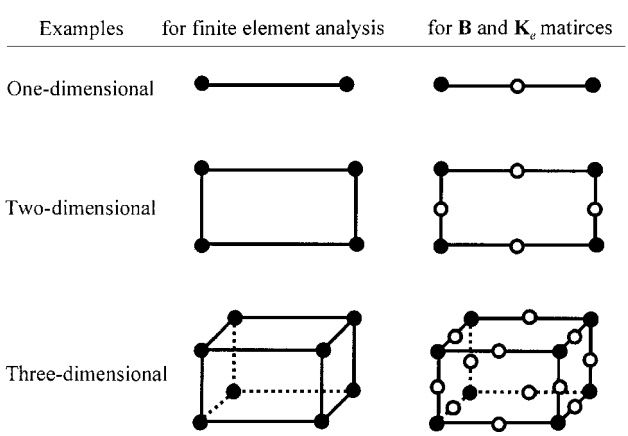

Fig. 1 Elements used for examples.

Example 1: One-Dimensional Problem

The equation of motion for a bar under axial load can be expressed as follows:

$$\frac{\mathrm{d}}{\mathrm{d}x}\left(EA\frac{\mathrm{d}u}{\mathrm{d}x}\right) + f = 0 \qquad \text{on} \qquad I = (0, 1) \tag{19}$$

with two boundary conditions,

$$u(0) = 0, \qquad u(1) = \bar{u} \tag{20}$$

where the extensional stiffness EA is set equal to 1 and the load vector f and the boundary displacement $\bar{u}$ are chosen such that the exact stress is given as

$$\sigma_{\text{exact}} = \left(EA\frac{\mathrm{d}u}{\mathrm{d}x}\right)_{\text{exact}} = 10x^2 - 5x + 5 \tag{21}$$

Two two-node linear elements are used to analyze this problem. In the ZZ method, a patch is constructed using two adjacent elements and a linear stress field is assumed over the patch because there is only one superconvergent point at each element. For the modified LP method, the stress is assumed as complete quadratic, as Eq. (2), over the same patch. In the present method, one three-node quadratic element is employed to construct the $\boldsymbol{B}$ and $\boldsymbol{K}_e$ matrices of each element for the stress recovery scheme. One superconvergent stress is calculated at each element center, and a quadratic stress field is assumed for the stress field within each element.

Figure 2 shows that the results obtained using the SP and the modified LP method agree well with the exact solution even at the boundaries, $x = 0$ and 1, whereas the ZZ method provides inaccurate boundary stresses. The values of α, β, and γ are set equal to 1, 1, and 0, respectively, in the SP method.

Example 2: Two-Dimensional Problem 1

An infinite plate with a center hole under unidirectional tensile stress is a popular two-dimensional example used in previous papers[7, 10, 11] because there exists an exact solution of the problem. The exact solution for the axial stress is given as the following:

$$\frac{\sigma_{xx}}{(\sigma_{xx})_\infty} = 1 - \frac{R^2}{r^2}\left(\frac{3}{2}\cos 2\theta + \cos 4\theta\right) + \frac{3}{2}\frac{R^4}{r^4}\cos 4\theta \tag{22}$$

The same example is chosen as the first example of two-dimensional problems. The problem is shown in Fig. 3. Because of the symmetry in the geometry and the applied load, only the shaded

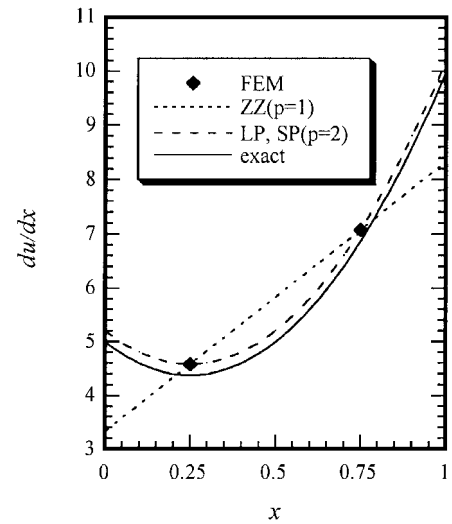

Fig. 2 Distribution of the axial stress, $EA(\mathrm{d}u/\mathrm{d}x)$ for $EA = 1$: example 1.

Table 1 Recovered boundary stresses, σ_{xx} (example 2)

Mesh	SP method $\alpha=1, \beta=1, \gamma=1$	SP method $\alpha=0, \beta=1, \gamma=1$	Exact, psi
1	2.6118 (12.94)[a]	2.6055 (13.15)	3
2	2.9430 (1.90)	2.9372 (2.09)	
3	3.0645 (2.15)	3.0615 (2.05)	
4	3.0681 (2.27)	3.0669 (2.23)	

[a]( ) indicates magnitude of relative error %.

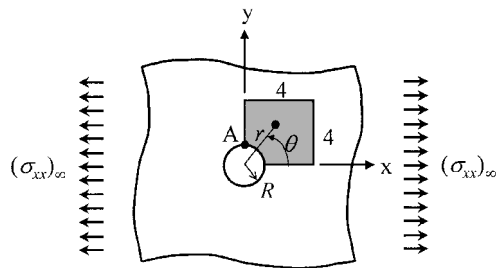

Fig. 3 Infinite plate with a center hole under uniform axial tension: $E = 10^7$ psi, $\nu = 0.3$, $(\sigma_{xx})_\infty = 1$ psi, $R = 1$ in., and thickness $t = 0.1$ in.

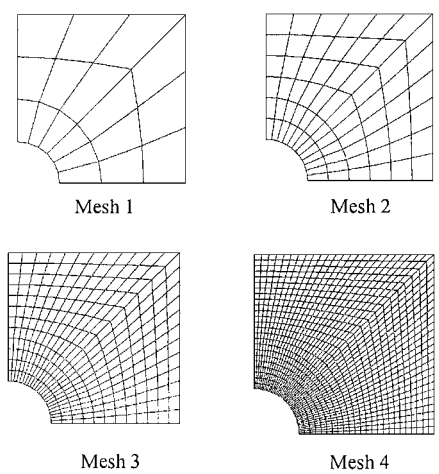

Fig. 4 Meshes used in example 2.

area is modeled using bilinear four-node plane stress elements. The equivalent traction forces are calculated and applied to the boundaries of the shaded area (along x and $y = 4$) to simulate the infinite plate. Proper symmetric boundary conditions are applied along the x and $y = 0$ boundaries. Four different meshes are used for the convergence check, and these meshes are shown in Fig. 4.

The bilinear stress field and the complete quadratic stress field are assumed for the three stress components over a patch in the ZZ method and the LP method, respectively. In the SP method, the complete quadratic stress for σ_{xx} [Eq. (5)] and bilinear stresses for the other two stress components [Eq. (4)] are assumed within an element because σ_{xx} is the dominant stress component in this example.

The axial stress at the boundary node point A in Fig. 3 is of interest in this example. First the performance of the SP method is checked. The recovered boundary stress using $\alpha = 0$, $\beta = \gamma = 1$ is compared with the result for $\alpha = \beta = \gamma = 1$ in Table 1. The two cases produced almost identical results for each mesh. This means that quite accurate boundary stresses can be recovered even without implementing the superconvergent stress.

Results from the different methods are compared with the result obtained by the SP method in Fig. 5. Figure 5 shows that the SP method provides a relatively accurate recovered stress at the boundary point A even for coarse meshes. All other methods provide worse boundary stresses when coarse meshes are used for the stress analysis.

Table 2 Recovered boundary stresses, σ_{xx} (example 3)

Mesh	SP method $\alpha=1, \beta=1, \gamma=1$	SP method $\alpha=0, \beta=1, \gamma=1$	Beam solution, psi
1	407.683 (5.64)[a]	407.683 (5.64)	432
2	432.096 (0.02)	432.096 (0.02)	
3	432.500 (0.12)	432.500 (0.12)	
4	434.176 (0.50)	434.176 (0.50)	

[a]( ) indicates magnitude of relative error %.

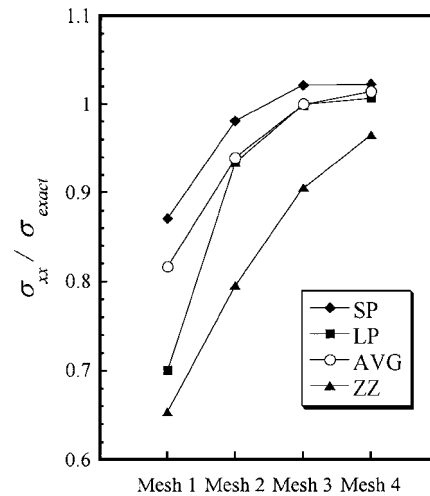

Fig. 5 Recovered axial stress at the point A: example 2.

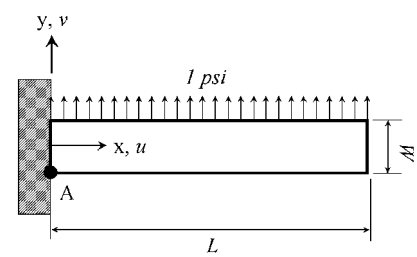

Fig. 6 Cantilever strip under uniform pressure: $E = 10^7$ psi, $\nu = 0.3$, $L = 12$ in., $W = 1$ in., and thickness $t = 0.25$ in.

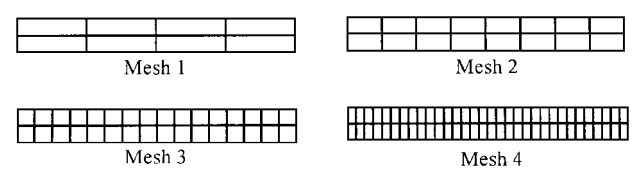

Fig. 7 Meshes used in example 3.

Example 3: Two-Dimensional Problem 2

Using the same plane stress element adopted in the preceding example, we analyzed a cantilever strip under uniform vertical pressure (shown in Fig. 6). Axial DOF (u) are restrained at the node points lying along the y axis, and the vertical DOF(v) is fixed only at $x = 0$ and $y = 0$. The same assumed stress field used in example 2 is employed for each method. Four different meshes (shown in Fig. 7) are used to check the convergence.

The axial stress at the boundary node point A in Fig. 6 is of interest in this example. For the SP method, the recovered boundary stress using $\alpha = 0$, $\beta = \gamma = 1$ is compared with the result for $\alpha = \beta = \gamma = 1$ in Table 2. Results from the two cases are identical for each mesh. This means that accurate boundary stresses can be recovered without the superconvergent stress information for the present in-plane bending problem. The beam solution in Table 2 indicates the solution based on Bernoulli–Euler beam theory. When this problem is modeled using 240×20 QUAD4 elements of MSC/NASTRAN, the boundary stress is calculated as $\sigma_{xx} = 437.54$ psi, which is very close to the beam solution.

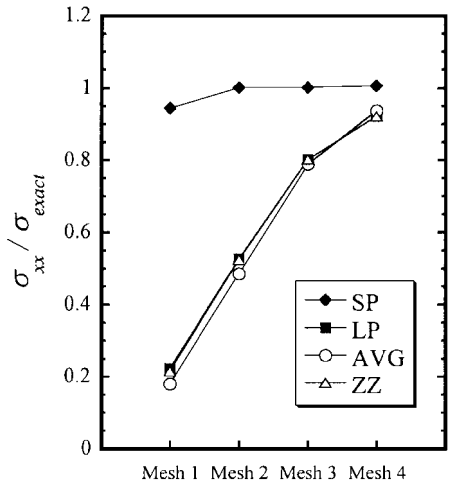

Fig. 8 Recovered axial stress at the point A: example 3.

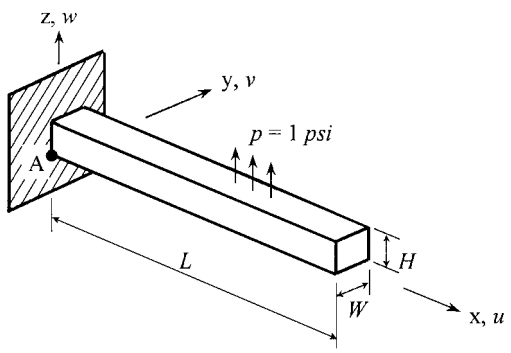

Fig. 9 Geometry and loading condition of a cantilever beam: $E = 10^7$ psi, $\nu = 0.3$, $L = 12$ in., $W = 1$ in., and $H = 1$ in.

Results from the different methods are compared with the result obtained by the SP method in Fig. 8. Figure 8 shows that the SP method can extract a very accurate stress at the boundary point A even for coarse meshes. All other methods provide only poor boundary stresses when coarse meshes are used for the stress analysis.

Example 4: Three-Dimensional Problem

A three-dimensional cantilever beam under uniform vertical pressure is modeled using eight-node three-dimensional sold elements. The geometry and the loading condition are shown in Fig. 9. All of the axial DOF(u) are restrained on the $x = 0$ surface. Lateral displacements (v) and vertical displacements (w) are fixed along z and y axes, respectively.

In the present method, the $\bar{\boldsymbol{P}}$ matrix for σ_{xx} is assumed as completely quadratic in (ξ, η, ζ) [as in Eq. (23)], and the trilinear stress fields [as in Eq. (24)] are assumed for the other five components within an element. For the ZZ method, the trilinear stress field is assumed for the axial stress over a patch. The same trilinear stress is assumed within an element for the AVG method. Six different meshes (shown in Fig. 10) are used to check the convergence characteristic of each method. Thus,

$$\bar{\boldsymbol{P}} = [1 \quad \xi \quad \eta \quad \zeta \quad \xi\eta \quad \eta\zeta \quad \xi\zeta \quad \xi^2 \quad \eta^2 \quad \zeta^2] \tag{23}$$

$$\bar{\boldsymbol{P}} = [1 \quad \xi \quad \eta \quad \zeta \quad \xi\eta \quad \eta\zeta \quad \xi\zeta \quad \xi\eta\zeta] \tag{24}$$

The axial stress σ_{xx} at the boundary node point A in Fig. 9 is of interest in this example. To check the performance of the SP method, the recovered boundary stress for $\alpha = 0$, $\beta = \gamma = 1$ is compared with the result for $\alpha = \beta = \gamma = 1$ in Table 3. Results from the two cases are almost identical for each mesh, as in the other examples. This implies that very accurate boundary stresses can be recovered without implementing the superconvergent stress for this three-dimensional bending problem. The beam solution in Table 3 indicates the solution based on Bernoulli–Euler beam theory. Modeling this problem

Table 3 Recovered boundary stresses, σ_{xx} (example 4)

Mesh	SP method $\alpha = 1, \beta = 1, \gamma = 1$	SP method $\alpha = 0, \beta = 1, \gamma = 1$	Beam solution, psi
1	357.638 (17.21)[a]	357.422 (17.26)	432
2	399.489 (7.53)	398.322 (7.80)	
3	426.243 (1.33)	424.251 (1.79)	
4	439.800 (1.81)	438.420 (1.49)	
5	445.220 (3.06)	444.714 (2.94)	
6	447.141 (3.50)	447.012 (3.48)	

[a]( ) indicates magnitude of relative error %.

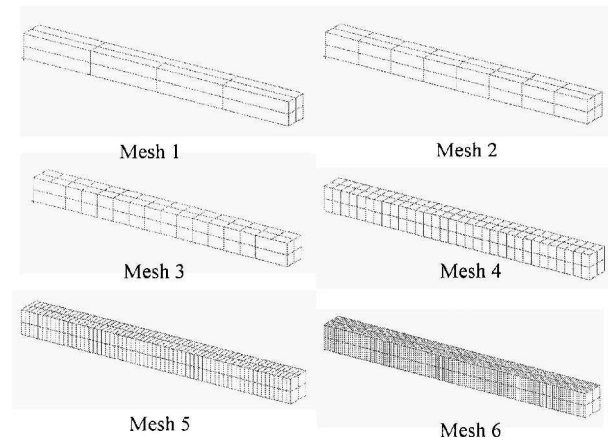

Fig. 10 Meshes used in example 4.

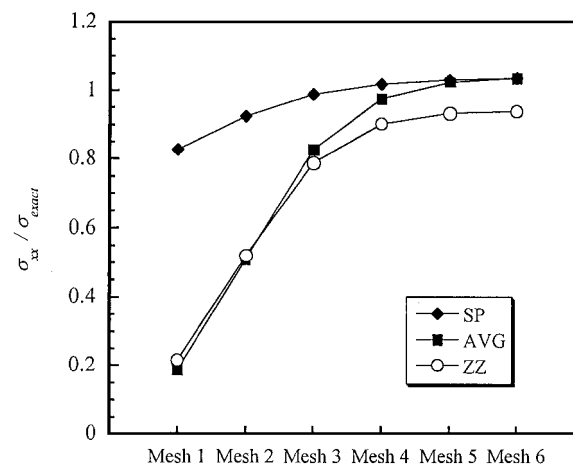

Fig. 11 Recovered axial stress at the point A: example 4.

using $60 \times 6 \times 6$ HEXA8 elements of MSC/NASTRAN, we obtained $\sigma_{xx} = 428.91$ psi, which is close to the beam solution.

The results obtained by the SP method are compared with the results from the order methods in Fig. 11. From Fig. 11, we can confirm that the SP method can extract a very accurate boundary stress at the point A even for coarse meshes, whereas other methods recover poor boundary stresses when coarse meshes are used for the stress analysis.

Conclusion

An element-base superconvergent stress recovery technique is developed for accurate boundary stress extraction. Numerical examples show that the method can recover quite accurate boundary stresses even without implementing the superconvergent stresses for two- and three-dimensional stress recovery problems. It is also observed that the element-base stress recovery can extract more accurate boundary stresses than the patch recovery approach can.

In the present method, the equilibrium constraint is imposed using two residuals of the equilibrium in variational forms. Inclusion of the two equilibrium residuals results in a stress recovery scheme that can recover accurate boundary stresses even for coarse meshes. The

recovery stress is assumed as higher order only for a dominant stress component. This selective higher-order stress assumption makes the present method able to extract very accurate boundary stresses even without implementing superconvergent stresses. The method should be very effective for the localized boundary stress recovery.

References

[1]Barlow, J., "Optimal Stress Locations in Finite Element Models," *International Journal for Numerical Methods in Engineering*, Vol. 10, No. 2, 1976, pp. 243–251.

[2]Zienkiewicz, O. C., and Zhu, J. Z., "A Simple Error Estimator and Adaptive Procedure for Practical Engineering Analysis," *International Journal for Numerical Methods in Engineering*, Vol. 24, No. 2, 1987, pp. 337–357.

[3]Hinton, E., and Campbell, J. S., "Local and Global Smoothing of Discontinuous Finite Element Functions Using a Least Squares Method," *International Journal for Numerical Methods in Engineering*, Vol. 8, No. 3, 1974, pp. 461–480.

[4]Oden, J. T., and Brauchli, H. J., "On Calculation of Consistent Stress Distributions in Finite Element Approximations," *International Journal for Numerical Methods in Engineering*, Vol. 3, No. 2, 1971, pp. 317–325.

[5]Babuska, I., and Miller, A., "The Post-Processing Approach in the Finite Element Method—Part 1: Calculation of Displacements, Stresses and Other Higher Derivatives," *International Journal for Numerical Methods in Engineering*, Vol. 20, No. 6, 1984, pp. 1085–1109.

[6]Zienkiewicz, O. C., and Zhu, J. Z., "The Superconvergent Patch Recovery and *a Posteriori* Error Estimates. Part 1: The Recovery Technique," *International Journal for Numerical Methods in Engineering*, Vol. 33, No. 7, 1992, pp. 1331–1364.

[7]Zienkiewicz, O. C., and Zhu, J. Z., "The Superconvergent Patch Recovery and *a Posteriori* Error Estimates. Part 2: Error Estimates and adaptivity," *International Journal for Numerical Methods in Engineering*, Vol. 33, No. 7, 1992, pp. 1365–1382.

[8]Wiberg, N. E., and Abdulwahab, F., "Patch Recovery Based on Superconvergent Derivatives and Equilibrium," *International Journal for Numerical Methods in Engineering*, Vol. 36, No. 16, 1993, pp. 2703–2724.

[9]Wiberg, N. E., Abdulwahab, F., and Ziukas, S., "Enhanced Superconvergent Patch Recovery Incorporating Equilibrium and Boundary Conditions," *International Journal for Numerical Methods in Engineering*, Vol. 37, No. 20, 1994, pp. 3417–3440.

[10]Blacker, T., and Belytschko, T., "Superconvergent Patch Recovery with Equilibrium and Conjoint Interpolant Enhancement," *International Journal for Numerical Methods in Engineering*, Vol. 37, No. 3, 1994, pp. 517–536.

[11]Lee, T., Park, H. C., and Lee, S. W., "A Superconvergent Stress Recovery Technique with Equilibrium Constraint," *International Journal for Numerical Methods in Engineering*, Vol. 40, No. 6, 1997, pp. 1139–1160.

[12]Boroomand, B., and Zienkiewics, O. C., "Recovery by Equilibrium in Patches (REP)," *International Journal for Numerical Methods in Engineering*, Vol. 40, No. 1, 1997, pp. 137–164.

S. Saigal
Associate Editor